Non-Isothermal Cold Crystallization Kinetics and Morphology of PET + SAN Blends

Renate M. R. Wellen, Marcelo S. Rabello

Department of Materials Engineering, Federal University of Campina Grande, PB, Brazil

Received 14 May 2009; accepted 7 October 2009
DOI 10.1002/app.31620
Published online 17 December 2009 in Wiley InterScience (www.interscience.wiley.com).

ABSTRACT: The influence of small amounts of poly(styrene-*co*-acrylonitrile) (SAN) on the non-isothermal cold crystallization behavior and morphology of poly(ethylene terephthalate) (PET) was investigated by dynamic-mechanical thermal analysis, differential scanning calorimetry (DSC), optical microscopy, and scanning electron microscopy. The results indicated that SAN had a limited solubility in the amorphous phase of PET although in a larger scale a phase separation occurred. The addition of 1 wt % of SAN promoted a significant reduction in the crystallization rate of PET, acting as an antinucleating agent. The kinetics parameters were determined applying both the Ozawa and Mo approaches. Mo's model described the crystallization evolution better than the Ozawa one because it is possible to analyze the kinetic parameters in similar range of crystallinity degrees. © 2009 Wiley Periodicals, Inc. J Appl Polym Sci 116: 1077–1087, 2010

Key words: non-isothermal cold crystallization; Ozawa; Mo; PET; SAN

INTRODUCTION

The market for PET blow-molded products is in constant growth and, as a consequence, a great interest for grades with suitable characteristics and improved properties is noted. In the manufacture of PET blow-molded products, first the polymer melt is injected into a cold mold to produce an amorphous preform. This preform is then reheated above the glass temperature of PET and, in the rubbery state, is submitted to a simultaneous blowing and stretching process.[1] The final product is both transparent and semi-crystalline, with suitable mechanical and barrier properties. The main problem that the industry faces in this process is the early crystallization of PET that frequently occurs during the reheating stage. This is named cold crystallization, and is observed visually as haze or even opacity in the preforms. When this occurs, the preform looses its elasticity in the rubbery state, turning the blow molding stage unfeasible as the final shape is not properly obtained.

It has been shown before that blending PET with other polymers may reduce the rate of crystallization.[2–4] Another approach to reduce the tendency of PET to crystallize is to add comonomers in the polymerization reactor, obtaining copolymers.[5,6] However, in all the examples shown above two disadvantages are evident: (i) when copolymers are produced, a change in the polymerization conditions has to be done, resulting in huge implications to the industry procedures, including a reduction in production versatility and an increase in costs; (ii) when blends are prepared, at least in the studies cited earlier, the second component is usually added in reasonably high concentrations—between 10 and 50 wt %, with many implications to mechanical and optical properties and also to processing conditions. From the practical point of view, it is highly desirable that any change in the material characteristics do not lead to a change in the manufacturing procedures.

In previous works,[7,8] the current authors reported the effect of polystyrene (PS) on the isothermal cold crystallization and morphology of PET. These studies showed that adding small amounts of PS caused a significant reduction on the rate of crystallization of PET, broadening the operating window of the blow molding process but with no reduction in the product properties. These studies were done under isothermal conditions and the kinetics was evaluated using the Avrami approach.

The present article expands the previous investigation, using this time the amorphous copolymer styrene-acrylonitrile (SAN) in blends with PET and applying non-isothermal conditions to study the crystallization behavior. This blend is known to be immiscible,[9] but the higher polarity of SAN in comparison to polystyrene may cause a change in the crystallization behavior of PET. Blending an

Correspondence to: M. S. Rabello (marcelo@dema.ufcg.edu.br).

Contract grant sponsor: CAPES.

amorphous polymer to a crystallizable one may cause a dramatic effect on the thermodynamic and kinetic parameters that control the crystallization of the crystalline polymer.[10] To provide a systematic control of crystallization, it is essential that the crystallization kinetics of a polymer blend is investigated in detail. The kinetic parameters of non-isothermal crystallization were determined by using the theories developed by Ozawa[11] and Mo.[12]

THEORETICAL BACKGROUND

In the study of non-isothermal crystallization using DSC, the heat released during crystallization is a function of temperature rather than time as in the case of isothermal crystallization. As a result, the relative crystallinity X_T can be formulated as:

$$X_T = \frac{\int_{T_0}^{T} \left(\frac{dH_c}{dT}\right) dT}{\Delta H_c} \tag{1}$$

where T_o and T are the onset of crystallization and an arbitrary temperature, respectively, dH_c is the enthalpy of crystallization released during an infinitesimal temperature range dT, ΔH_c is the total enthalpy of crystallization for a specific heating/cooling condition.

To use eq. (1) in the analysis of non-isothermal crystallization data obtained by DSC, it is assumed that the sample experiences the same thermal history as designated by DSC furnace. This is achieved only when the temperature lag between the sample and the furnace is kept at a minimal.[13] If this assumption is valid then the relation between the crystallization time t and the sample temperature T can be taken as:

$$t = \frac{T_0 - T}{\varphi} \tag{2}$$

where φ is the heating/cooling rate.

According to eq. (2), the temperature axis observed in a DSC thermogram for the non-isothermal crystallization data can be transformed into the time scale.

The most common approach to describe the overall isothermal crystallization is the Avrami theory,[14] in which the relative crystallinity as a function of time can be expressed in the following form:

$$1 - X_t = e^{-Kt^n} \tag{3}$$

where n is the Avrami exponent, which depends on the nature of the nucleation and growth geometry of the crystals.

K is the crystallization rate constant, which depends on the nucleation and growth rates.

On the basis of a mathematical derivation, Ozawa[11] extended the Avrami theory to describe the non-isothermal crystallization by assuming that the sample was heated with a constant rate from the glassy state (or cooled from the melt). In the Ozawa theory, the time variable in the Avrami equation was replaced by a heating/cooling rate and the relative crystallinity as function of constant heating/cooling rate φ is:

$$X_T = 1 - \exp\left(-\left(\frac{K_{(T)}}{\varphi^m}\right)\right) \tag{4}$$

where m and $K_{(T)}$ are the Ozawa exponent and the Ozawa crystallization rate constant, respectively. Both parameters hold a similar meaning to those of the Avrami approach.

Analytically, the kinetic parameters can be obtained from a least-squared line drawn through the bulk of the data, according to the plot of $\mathrm{Ln}[-\mathrm{Ln}(1 - X_T)]$ versus Log φ for a fixed temperature, in which $K_{(T)}$ and m can be determined from the y-intercept and the slope, respectively.

To find a method to describe exactly the non-isothermal crystallization process, Mo et al.[12] developed a novel kinetic approach by combining the Avrami equation [eq. (3)] with the Ozawa equation [eq. (4)] as follows:

$$\mathrm{Log}\ K + n\ \mathrm{Log}\ t = \mathrm{Log}\ K_{(T)} - m\ \mathrm{Log}\ \varphi \tag{5}$$

$$\mathrm{Log}\ \varphi = \frac{1}{m}\mathrm{Log}\left[\frac{K_{(T)}}{K}\right] - \frac{n}{m}\mathrm{Log}\ t \tag{6}$$

Taking

$$F_{(T)} = \left[\frac{K_{(T)}}{K}\right]^{1/m} \quad \text{and} \quad a = \frac{n}{m}$$

The final form of Mo equation is:

$$\mathrm{Log}\ \varphi = \mathrm{Log}\ F_{(T)} - a\ \mathrm{Log}\ t \tag{7}$$

where $F_{(T)}$ is a parameter which is dependent on the heating rate and a is the ratio between Avrami and Ozawa exponents.

The kinetic parameters are obtained from a least-squared line drawn through the bulk of the data in the plot of Log φ versus Log t at a given crystallinity degree, whereas Log $F_{(T)}$ and a can be determined from the y-intercept and the slope, respectively.

EXPERIMENTAL

Materials

PET (bottle grade) was supplied by Rhodia-Ster (Rhopet S78), with an intrinsic viscosity [η] of

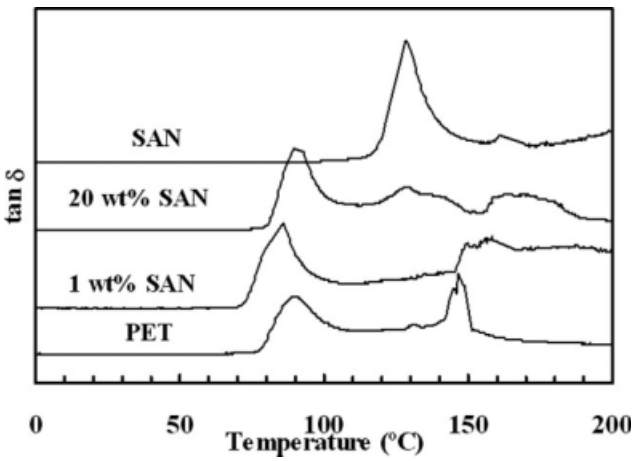

Figure 1 DMTA analysis of PET, SAN, and the blends.

0.78 dL/g and M_w = 48,000 g/mol. The copolymer of styrene and acrylonitrile (SAN) was Basf Luran 358N that is normally used for injection molding. Both polymers were used as received and no information was given by the producers regarding the additives present in them.

Compounding

Before mixing, the polymers were previously dried in the oven with forced air circulation. PET was dried at 120°C for 6 h to avoid hydrolysis during processing, and SAN was dried at 80°C for 14 h to remove moisture. The compounding was conducted in a torque rheometer System-90 of Haake-Büchler coupled with the internal mixer Rheomix 600, operating with rotors of roller type. The mixture was done at 265°C and 60 rpm, during 10 min using 50 grams of material. After compounding, the melt was quickly quenched in water/ice to obtain amorphous blends. This procedure was used for both neat PET and the blends. The samples for DMA and SEM were obtained by hand pressing the melt material between spatulas while quenching.

Sample characterization

Measurements of loss factor (tan δ) were obtained using a DMA 983 (TA Instruments) equipment by heating the amorphous samples from −20 to 200°C, with a frequency of 1 Hz and heating rate of 2°C/min, under nitrogen.

Differential scanning calorimetry measurements were carried out in a Shimadzu DSC-50 equipment. Glassy samples were heated from room temperature to 300°C, using heating rates ranging from 1 to 50°C/min. From the thermograms the thermal parameters were obtained and the analysis of crystallization kinetics was conducted, following the theoretical background shown before.

Scanning electron microscopy (SEM) analyzes were done in a Shimadzu SSX 550 Superscan. The samples were fractured in liquid nitrogen and covered with gold to avoid charging. Polarized light microscopy analyzes were done with an Olympus B201. The samples were placed between glass sheets and heated to 270°C; the sheets were then quickly quenched in water/ice to produce amorphous samples. The morphology developed during the cold crystallization was analyzed using a heating rate of 10°C/min.

RESULTS AND DISCUSSION

Dynamic-mechanical thermal analysis

The Dynamic-mechanical thermal analysis (DMTA) results of tan δ for SAN, PET, and the blends with 1 and 20 wt % SAN are presented in Figure 1. This property is related to the ability of the sample to dissipate energy and the peak position is considered as the most appropriate method to measure the glass transition temperature of polymers.[15] From Figure 1, it is clear that the peaks position corresponding to the glass transitions of PET and SAN are not affected in the blends when compared to the pure polymer, indicating that the two components are immiscible. Other humps that appear in the thermograms may be artefacts of sample analysis, due to, for instance, sample slipping at the grips. For the sample with 1% wt SAN the peak related to the T_g of SAN did not appear due to the low content of this component.

Non-isothermal cold crystallization

DSC scans for PET and for the blends with 1, 15, and 20 wt % SAN are shown in Figure 2. The addition of SAN caused a displacement of the

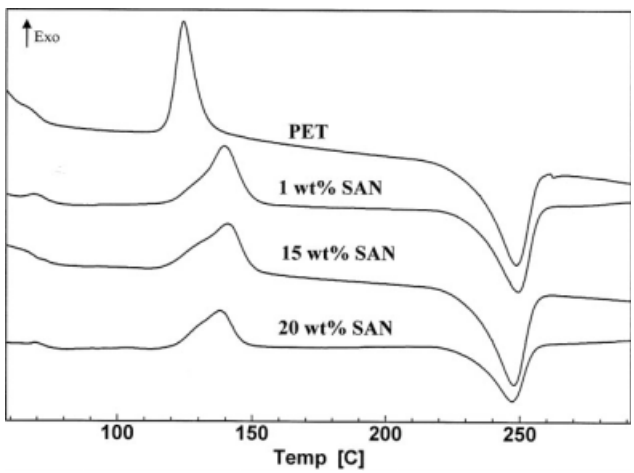

Figure 2 DSC scans for PET and PET + SAN blends using a heating rate of 10°C/min.

crystallization exotherms toward higher temperatures. Somewhat similar behavior was observed in other combinations, like PEO + PES[16] and PET + PC.[17] The crystallization shift with 1% SAN in Figure 2 was quite significant (~ 15°C) but further increases in SAN concentration did not promote more displacement in the crystallization range of PET. This is rather similar to what was reported before by the present authors for PET + PS blends[8] in isothermal conditions. Although PET + SAN blends are essentially immiscible (see the SEM analyzes later), it is possible that a very small fraction of SAN molecules is actually soluble in the amorphous phase of PET. This consideration is based on the concept of solubility, where traces of a component can be soluble in a medium even without forming an homogeneous mixture (where the solute is present in larger proportions).[18] In the case of PET + SAN mixtures, the solubility limit of SAN in PET must be low (certainly less than 1 wt %, as phase separation was observed with this concentration[19]), but it is able to hinder the crystallization of PET. No data from the literature was obtained about the solubility of this pair of polymers, however. The existence of a low solubility limit explains the little influence of higher concentrations of SAN in the cold crystallization of PET. The use of only 1 wt % of SAN to increase the temperature of cold crystallization of PET in a similar way to what was obtained with much higher concentrations, highlights the importance of the current investigation. In this concentration, no significant effects were detected in the mechanical and optical properties of PET.[19] In addition, the procedures for industrial application of these blends, in the manufacture of bottles and thermoformed products for example, are quite simple and require no change in comparison to the processing of neat PET. From these results the blend with 1 wt % SAN was selected for a more detailed study.

From dynamic DSC heating experiments the crystallization exotherms as a function of temperature are obtained for various heating rates, as shown in Figure 3 for PET and for the blend with 1 wt % SAN. A displacement of the crystallization exotherm to higher temperatures is observed when the heating rate is increased. The cold crystallization temperature range depends on the magnitude of the nucleation and crystalline growth rates; for high heating rates less time is available for crystallization and, therefore, the whole process is delayed to higher temperatures. It is also observed in Figure 3 that the exotherms of the blends with SAN occurred at higher temperatures when compared to the ones obtained with the pure PET. This was observed in all heating rates and confirms the observation made before that the presence of SAN, even in very small amounts, reduced the crystallization rate of PET.

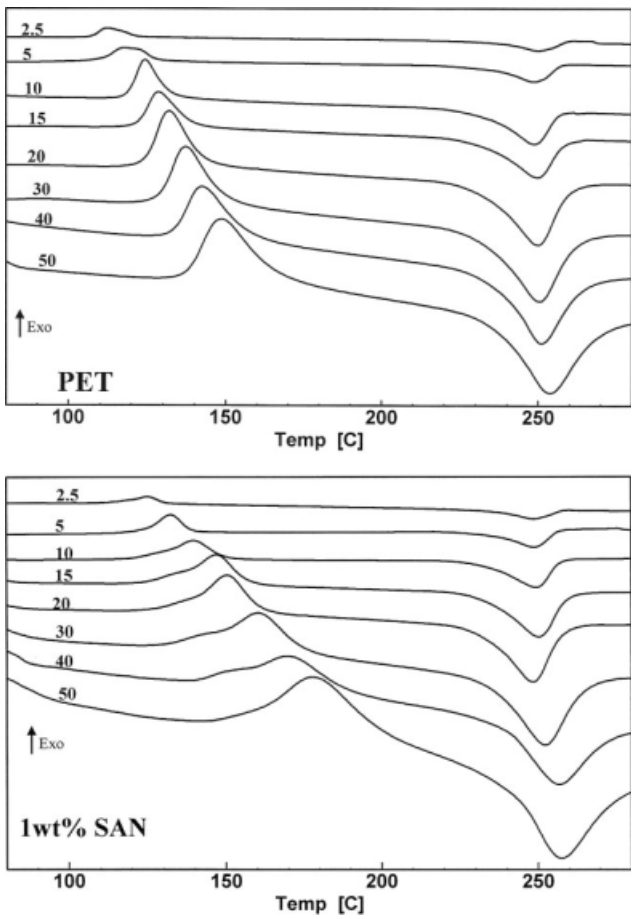

Figure 3 Selected DSC scans for PET and for the blend with 1 wt % SAN. The heating rates (in °C/min) are indicated.

Also from Figure 3, the melting endotherms of PET seemingly did not present significant changes with the different heating rates used or with the addition of SAN, i.e., the differences in T_m among the various samples and conditions were less than 1°C.

The temperature range for non-isothermal crystallization (ΔT_c), taken as the difference between the starting and the ending of cold crystallization in DSC heating thermograms, can be considered as an indicative of the crystallization rate; higher T_c and wider ΔT_c imply that PET has more difficulty to cold crystallize. The results of Figure 4 show an increase in T_c and ΔT_c with increasing heating rate. Moreover, for all heating rates PET presented values of T_c and ΔT_c lower than those obtained with the blends with SAN, suggesting that in the neat polymer a smaller amount of energy is necessary for the relaxation of the amorphous fraction, facilitating the cold crystallization. The increase in T_c and ΔT_c in the blends can be ascribed to the reduction of the crystallizability of the molecules due to the presence of the non-crystallizable component.[20]

According to Beck et al.[21] the nucleation rate (N) can be taken as the tangent of the linear part of

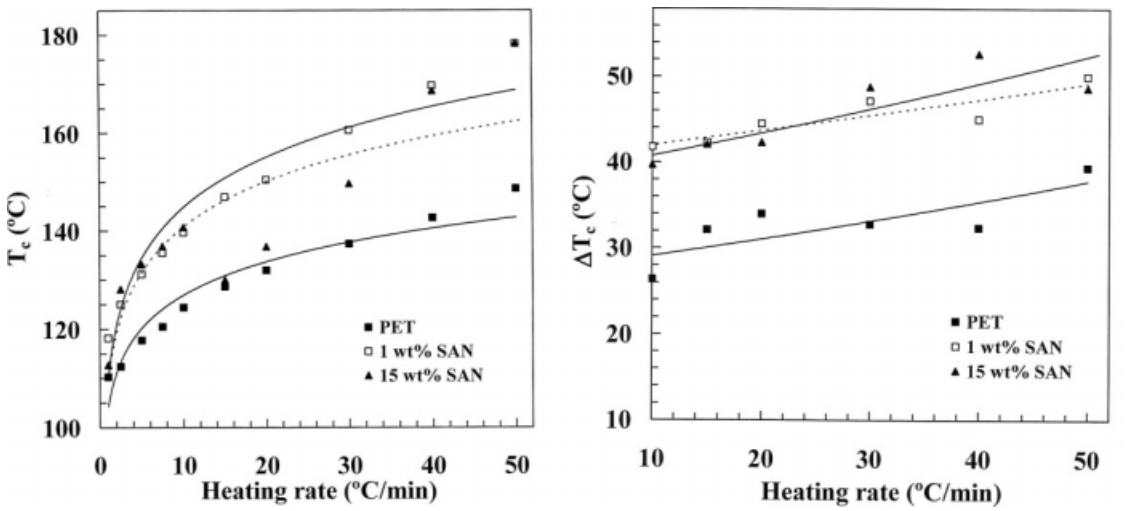

Figure 4 Effect of heating rate on the crystallization temperature (T_c) and crystallization range (ΔT_c) observed during non-isothermal cold crystallization of PET and blends with SAN.

starting of crystallization exotherm. This procedure was done for PET and PET + SAN blends using the exotherms of Figure 3 and the results are given in Figure 5. The nucleation rate increased with the heating rate and all values were higher for PET than for the blends. It is remarkable that only 1% of SAN promoted such a significant reduction in the nucleation rate of PET, which can be associated to an existence of limited solubility between PET and SAN, as discussed before. An increase in the energy necessary for the formation of the nucleus as well as bigger crystalline entities (see Fig. 12 latter on) should result in a lower nucleation rate.[22] Because of this significant reduction in N the copolymer SAN can be considered as an "antinucleating agent"[8] on the cold crystallization process of PET in contrast to the nucleating agents that increase the nucleation rate of polymers.

Compounds used to reduce the crystallization rate of PET are scarce in the literature; examples of these agents are THP comonomer,[5] SSBA sodium salt,[23] and nanosilica.[24] However, in these cases a high amount of the second component had to be added to obtain a reasonable reduction in the crystallization rate, and this high concentration might cause a negative effect in the properties and processabillity of PET. In the current work, the great technological and scientific interest comes from the fact that the extraordinary reduction in the nucleation rate was obtained with the addition of only 1% of SAN, with minimum influences in the optical and mechanical behavior of PET.[19]

Kinetics of non-isothermal cold crystallization—Ozawa theory

From DSC scans shown in Figure 3 the relative crystallinity development with temperature, X_T, was calculated and the "S-shaped" curves were obtained (Fig. 6). The relative crystallinity is calculated as the ratio between the crystallinity at a certain condition and the maximum crystallinity achieved. The final value, therefore, equal to the unity. These curves are shifted to higher temperatures with increasing heating rates, following the displacement of the exotherms (Fig. 3). In Figure 6, it is also noted that the "S-shaped" curves of the blends are dislocated to higher temperatures, indicating that SAN turns the crystallization of PET slower. From these curves the plots $\mathrm{Ln}[-\mathrm{Ln}(1-X_T)]$ versus $\mathrm{Ln}[1/(dT/dt)]$ were constructed (Fig. 7) and the Ozawa parameters, m and K_T, were estimated from the slope and intercept,

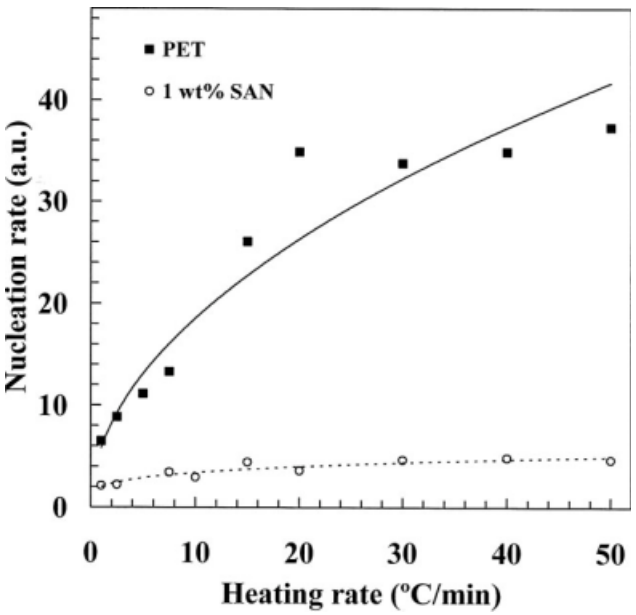

Figure 5 Effect of heating rate on the nucleation rate of PET and its blend with 1 wt % SAN.

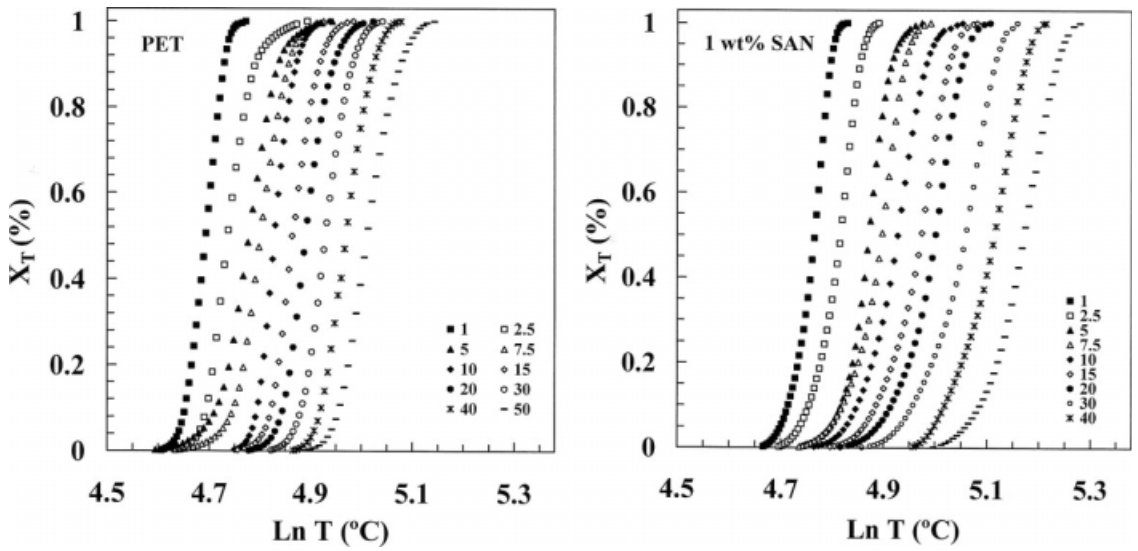

Figure 6 Development of crystallinity (X_T) with temperature during non-isothermal cold crystallization of PET and the blend with 1 wt % SAN at different heating rates (as indicated, in °C/min).

respectively (Table I). The rate constant K_T showed a variable tendency according to the compound tested. For neat PET, K_T decreased systematically with increasing crystallization temperature, whereas for the blends with 1% SAN the opposite trend was observed. For blends with a higher SAN content, K_T decreased initially with increasing crystallization temperature reaching the lowest value at $\sim$ 130°C; an opposite tendency was observed with isothermal conditions.[25,26] These various tendencies may result from the limitations of the method and this will be referred again later on in this article. It is also observed in Table I that for most temperatures K_T showed lower values for the blends, following the tendency obtained with PET + PS during the isothermal cold crystallization.[8] The Ozawa exponent m reduced with increasing the temperature. At low temperatures the crystalline growth rate is lower, favoring the development of more complex morphologic structures.

According to Hieber,[27] a rate constant Z can be calculated using the Ozawa parameters [eq. (8)]. Using the Z constant, the results obtained for crystallization in isothermal and non-isothermal conditions are analyzed jointly.

$$Z = K_{(T)}{}^{1/m} \tag{8}$$

Figure 8 shows that an increase in Z with increasing the crystallization temperature is observed for both PET and blends, following the same tendency observed previously during isothermal cold crystallization of PET + PS.[8] Similar behavior was noted in various systems, including PES[28] and PET.[29]

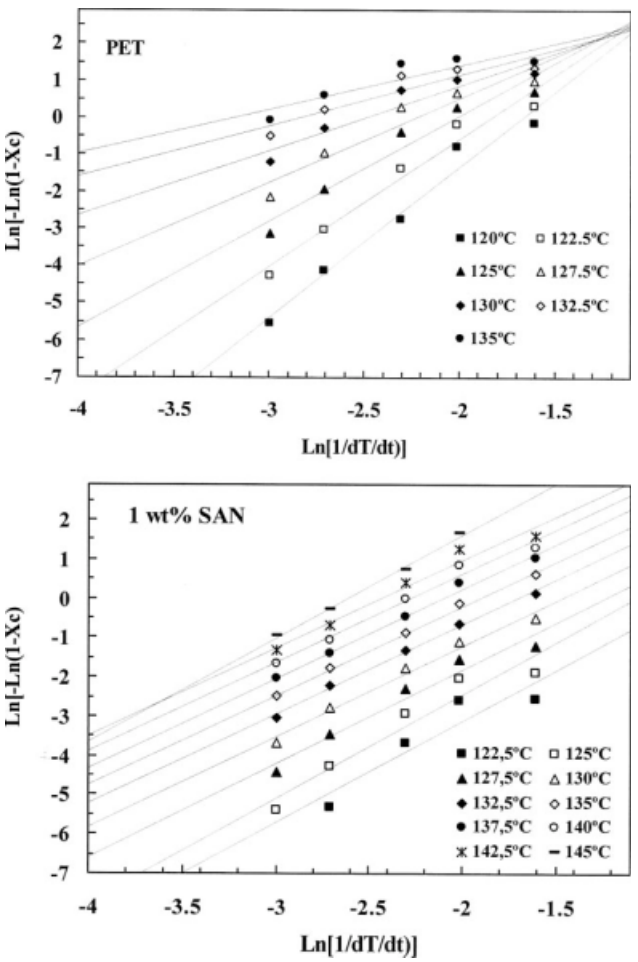

Figure 7 Plots of Ln[−Ln(1 − X_T)] versus Ln[1/(dT/dt)] of PET and the blend with 1 wt % SAN at different crystallization temperatures.

TABLE I
Kinetic Parameters of Ozawa Equation for the First Stage OF Non-Isothermal Cold Crystallization of PET and PET + SAN Blends

	PET		1 wt % SAN		15 wt % SAN		20 wt % SAN	
T_c (°C)	m	K_T (10^{-3}/min)	m	K_T (10^{-3}/min)	m	K_T (10^{-3}/min)	m	K_T (10^{-3}/min)
120	4.1	881.1	–	–	3.0	26.7	3.6	93.3
122.5	3.5	549.8	2.6	7.7	2.4	15.3	3.2	75.4
125	2.9	314.5	2.6	17.5	2.0	11.5	2.8	69.6
127.5	2.2	158.3	2.4	19.6	1.6	8.4	2.5	66.4
130	1.8	80.0	2.3	29.8	1.4	6.8	2.5	107.9
132.5	1.4	49.4	2.3	48.8	1.2	7.0	2.2	84.1
135	1.2	44.0	2.3	77.3	1.2	8.8	2.0	91.3
137.5	–	–	2.3	122.3	1.2	12.6	1.9	95.9
140	–	–	2.3	168.7	1.3	23.5	1.8	108.2
142.5	–	–	2.3	231.4	1.2	28.4	–	–

Comparing PET + SAN with neat PET, it is observed that the blends presented a significant reduction in the crystallization rate for all crystallization temperatures, which is consistent with the previous results.

According to the results presented earlier, the Ozawa theory can provide very useful information on the kinetics of non-isothermal cold crystallization of PET. However, an analysis of its experimental and theoretical limitations is necessary. Although the Ozawa theory simplifies the crystallization process, considering it as a uniform phenomenon, the dynamic crystallization involves many complexities that depend on the magnitude of the nucleation and growth stages and these vary with the crystallization temperature.[30] During non-isothermal crystallization, therefore, the polymer is submitted to various effects with a change in temperature and time that does not necessarily follow the same tendency for isothermal crystallization conditions.

Kinetics of non-isothermal cold crystallization—Mo theory

The horizontal temperature axis of Figure 6 was converted into time scale by applying eq. (2) and the relative crystallinity development with time $X_{t'}$ for non-isothermal crystallization was plotted as shown in Figure 9. The higher the heating rate, the shorter is the time to finish crystallization. From the curves of Figure 9 the parameters $t'_{0.5}$ and $C'_{0.5}$, representing respectively the time to reach 50% of crystallinity and the crystallization rate (taken as the inverse of $t'_{0.5}$) were estimated and the results are given in Figure 10. $t'_{0.5}$ decreased exponentially with heating rate and the blend presented higher crystallization times for all the heating rates, since the presence of the SAN delays the non-isothermal crystallization of PET. Following the inverse trend, the crystallization rate was slower in the blends.

The values of X_t were analyzed by using the usual double logarithmic form [eq. (3)] and are presented in Figure 11. Each curve shows two regions: an initial linear portion (usually called the primary stage), followed by a leveling off (the secondary stage). It is also noted that the time interval for the secondary stage decreases with increasing heating rate, agreeing with the decrease in the curvature of the $X_{t'}$ curves observed in Figure 9.

The Avrami exponent n' and the rate parameter $K'_{(T)}$ for the non-isothermal cold crystallization of PET and of the blend with SAN were estimated from the slope and intercept, respectively, in the plot of $\log[-\mathrm{Ln}(1 - X_{t'})]$ versus Logt (Fig. 11) and the results are displayed in Table II. The values of the exponent n' were approximately of two for both PET and blends, associated with a growth in disk form generated by heterogeneous nucleation. The

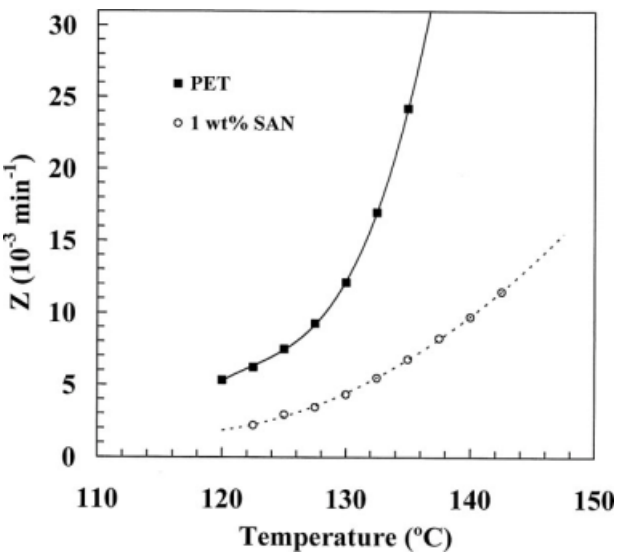

Figure 8 Effect of the crystallization temperature on the rate constant Z of PET and its blend with 1 wt % SAN during non-isothermal cold crystallization.

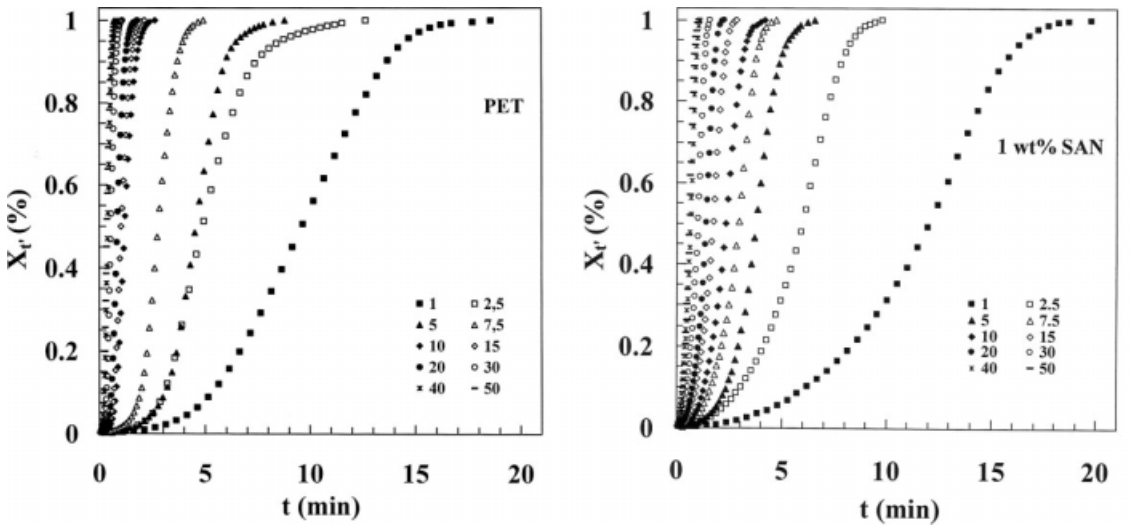

Figure 9 Development of crystallinity with time for non-isothermal cold crystallization of PET and the blend with 1 wt % SAN at different heating rates (as indicated, in °C/min).

rate constant $K'_{(T)}$ increased with heating rate and decreased with the presence of SAN.

Plots of Log t versus Log φ for several conversion degrees were constructed (not shown here) and the parameters a and $F_{(T)}$ were determined and displayed in Table III. The values of a were close to 1 for PET and for the blends, whereas $F_{(T)}$ increased systematically with increasing relative crystallinity, indicating that at a given crystallization time, a higher heating rate should be used in order to obtain a higher crystallinity degree. The $F_{(T)}$ parameter can also be considered as a parameter for the non-isothermal crystallization rate. Lower values of $F_{(T)}$ indicate that the non-isothermal crystallization occurred in an accelerated way.[31] As shown in Table III, the $F_{(T)}$ values for the blends were higher than those for neat PET, confirming that the blends had a slower crystallization rate than PET.

The Mo theory described successfully the non-isothermal cold crystallization behavior of PET and PET + SAN blends as observed above. In our opinion, this approach is better than the one proposed by Ozawa, where an anomalous behavior was observed in the $K_{(T)}$ constant (Table I). In the theory of Ozawa, the kinetic analysis is carried out in different temperature ranges and, therefore, the kinetics parameters are determined in different crystallinity degrees. This can lead to some inconsistencies, like in conditions where some samples may be in the beginning of the crystallization while others at the end.

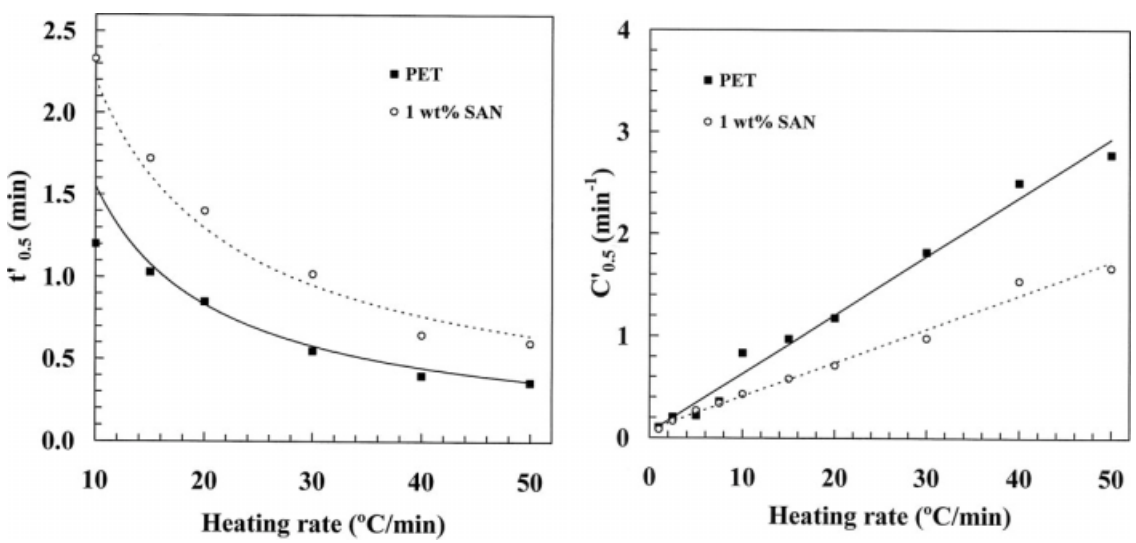

Figure 10 Effect of heating rate on half time of crystallization and on crystallization rate of PET and its blend with 1 wt % SAN.

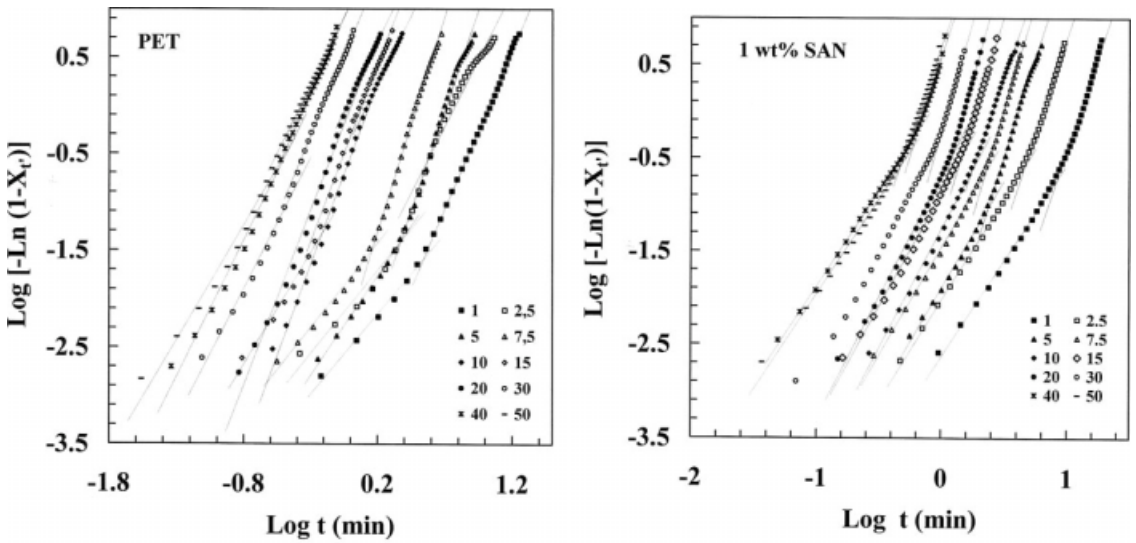

Figure 11 Plots of $\log[-\mathrm{Ln}(1 - X_{t'})]$ versus Logt for PET and the blend with 1 wt % SAN at different heating rates (as indicated, in °C/min).

This causes a great heterogeneity on the physical state of the samples. The great advantage of using the Mo theory is that it makes possible the analysis of the kinetic data in similar range of crystallinity degrees.

Optical microscopy analysis

Figure 12 displays light optical microscopy images of PET and the blend with 1 wt % SAN after cold crystallization. PET presents a larger number of crystalline domains whereas in the blend the domains are much larger. Even though in both situations the spherulites are not fully developed and, with the magnification provided, not well defined, these birrefringent structures are actually crystalline domains, as already observed by others with PET compounds.[32] The difference in sample morphology shown in Figure 12 is in agreement with the decrease in the nucleation rate of PET when SAN is present (Fig. 5).

The size of the crystalline entities depends on the nucleation and crystalline growth rates and these are related to the molar mass and to the chemical regularity of the macromolecules.[33] It is possible that the addition of a non-crystallizable polymer like SAN to PET contributes to the decrease in the regularity of the molecules and reduces the crystallizabillity of PET, reducing the nucleation rate of the blends. A decrease in the nucleation rate and subsequent increase in the crystalline entities was observed before in many systems, like in photo-degraded PP[34] and in PET containing manganese.[35]

SEM analysis

For SEM analysis a blend with 15 wt % SAN was selected to favor a better visualization the

TABLE II
Kinetic Parameters of Avrami-Ozawa Equation for Non-Isothermal Cold Crystallization of PET and PET + SAN Blends

Heating rate (°C/min)	PET		1 wt % SAN		15 wt % SAN	
	n'	$K'_{(T)}$	n'	$K'_{(T)}$	n'	$K'_{(T)}$
5	2.3	6.7	2.3	12.7	2.1	38.2
7.5	2.0	19.6	2.2	33.2	2.2	40.0
10	3.3	202.0	2.4	51.1	2.2	68.7
15	2.7	233.2	2.3	115.0	2.5	266.2
20	3.1	525.3	2.4	170.6	2.2	303.7
30	2.6	1502.5	2.3	437.4	2.1	471.8
40	2.5	3299.9	2.1	1488.0	2.1	1020.0
50	2.2	2817.7	1.9	924.7	1.8	791.4

Parameters determined for conversion degree $(X_{t'})$ of 10% in the first stage of crystallization.

TABLE III
Mo Parameters for Non-Isothermal Cold Crystallization of PET and PET + SAN Blends

X_T (%)	PET		1 wt % SAN		15 wt % SAN	
	a	$F_{(T)}$	a	$F_{(T)}$	a	$F_{(T)}$
10	0.79	12.3	0.93	19.9	0.94	13.2
20	0.81	14.1	1.00	23.3	0.97	16.4
30	0.82	15.3	1.06	27.5	0.98	19.2
40	0.84	16.4	1.09	30.7	0.99	21.7
50	0.85	17.5	1.11	33.3	0.99	24.1
60	0.86	18.7	1.12	35.7	1.02	27.1
70	0.87	20.1	1.13	38.1	1.04	30.2
80	0.88	21.7	1.15	40.9	1.07	33.9
90	0.90	24.2	1.15	44.3	1.11	38.8

morphology, as the one with only 1% of SAN the second phase is hardly seen. In Figure 13, a two-phase structure which is composed of PET matrix and SAN domains is clearly noticed. It is also observed that some domains of SAN remained adhered to PET matrix after fracture, due to existence of some interaction between the phases. These interactions occur due to a polar character of SAN that generates electronic dipoles with the chemical groups of PET. The medium diameter (d_m) of the dispersed domains of SAN was calculated as 1.2 μm. This image is rather different from the one obtained with PET + PS blends in a previous study,[8] where very clear separation between the phases, low adhesion and also a much higher domain diameter (d_m = 2.4 μm) were observed.

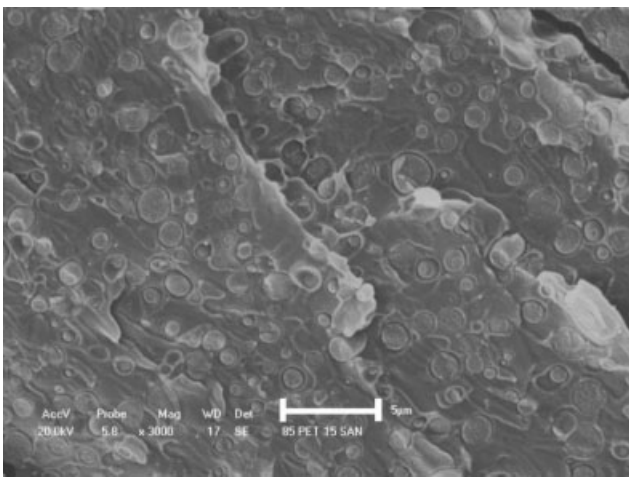

Figure 13 SEM image for the blend with 15 wt % SAN (scale bar: 5 μm).

CONCLUSION

The non-isothermal cold crystallization of PET and PET + SAN blends was analyzed in detail. The presence of SAN significantly reduced the cold crystallization rate of PET and promoted a decrease in the nucleation rate. These effects were observed even when only 1 wt % of SAN was added. This is the same tendency observed previously with polystyrene when the investigation was done under isothermal conditions.[8] Therefore, SAN can also be considered as an "anti-nucleating" additive to PET but with a better adhesion to the matrix when compared to the polystyrene particles. From the technological point of view the fact that the addition of only 1 wt % of SAN can reduce the cold crystallization rate of PET is highly important as a broadening the operating window during blow molding processing is achieved, reducing manufacture scrap due to premature crystallization.

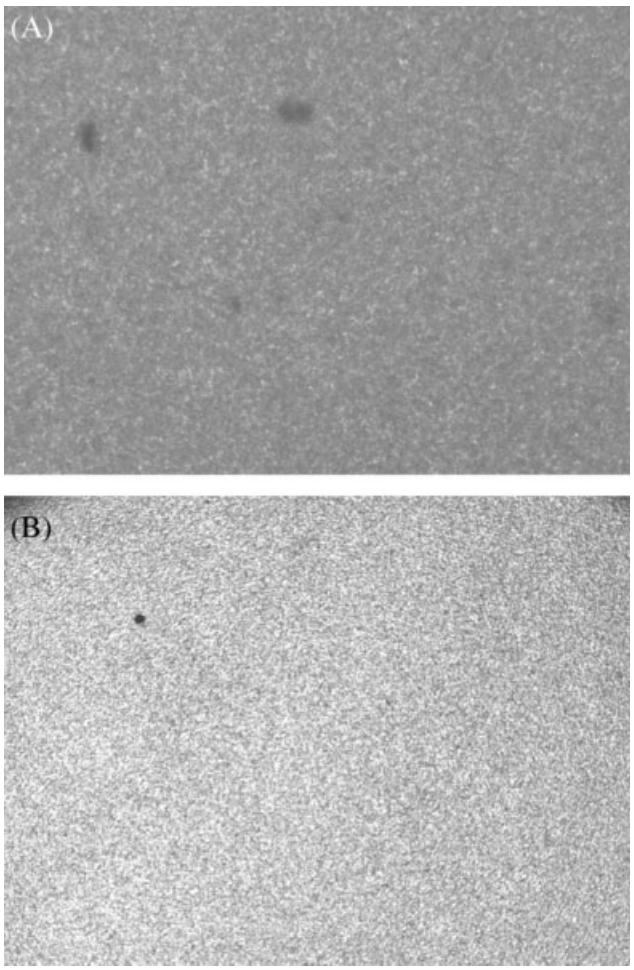

Figure 12 Optical microscopy images of neat PET (A) and blend with 1 wt % SAN (B) after cold crystallization.

The authors would like to thank Maria Isabel Felisberti (UNICAMP-Brazil) for DMTA analysis.

References

1. Griskey, R. G. Polymer Processing Engineering; Chapman & Hall: New York, 1995.
2. Rahman, M. R.; Nandi, A. K. Polymer 2002, 43, 6863.
3. Tang, S. D.; Xin, Z. Polymer 2009, 50, 1050.
4. Liang, H.; Xie, F.; Guo, F. Q.; Chen, B.; Luo, F. S.; Jin, Z. Polym Bull 2008, 60, 115.
5. Connor, D. M.; Allen, S. D.; Collard, D. M.; Liotta, C. L.; Schiraldi, D. A. J Appl Polym Sci 2001, 80, 2696.
6. Kint, D. P. R.; Ilarduya, A. M.; Sansalvadó, A.; Ferrer, J.; Muñoz-Guerra, S. J Appl Polym Sci 2003, 90, 3076.
7. Wellen, R. M. R.; Rabello, M. S. Polímeros: Ciências e tecnologia 2007, 17, 113.
8. Wellen, R. M. R.; Rabello, M. S. J Appl Polym Sci 2009, 114, 1884.
9. Oyama, H. T.; Kitagawa, T.; Ougizawa, T.; Inoue, T.; Weber, M. Polymer 2004, 45, 1033.
10. Paul, D. R.; Barlow, J. W. J Macromol Sci Rev Macromol Chem Phys 1980, c18, 109.
11. Ozawa, T. Polymer 1971, 12, 150.
12. Liu, T.; Mo, Z.; Wang, S.; Zhang, H. Polym Eng Sci 1997, 37, 568.

13. Achilias, D. S.; Papageorgiou, G. Z.; Karayannidis, G. P. J Polym Sci Part B: Polym Phys 2004, 42, 3775.
14. Avrami, M. J Chem Phys 1939, 7, 1103.
15. Campbell, D.; White, J. R. Polymer Characterization: Physical Techniques; Chapman & Hall: London, 1989.
16. Dreezen, G.; Fang, Z.; Groeninckx, G. Polymer 1999, 40, 5907.
17. Kong, Y.; Hay, J. N. Polymer 2002, 43, 1805.
18. Olabisi, O.; Robeson, L. M.; Shaw, M. T. Polymer-Polymer Miscibility; Academic Press: New York, 1979.
19. Wellen, R. M. R. Ph.D. Thesis, Federal University of Campina Grande, Brazil, 2007.
20. Keith, H. D.; Padden, F. J., Jr. J Appl Phys 1964, 35, 1270.
21. Beck, H. N.; Ledbetter, H. D. J Appl Polym Sci 1965, 9, 2131.
22. Connor, D. M.; Allen, S. D.; Collard, D. M.; Liotta, C. L.; Schiraldi, D. A. J Appl Polym Sci 2001, 81, 1675.
23. Kang, H.; Lin, Q.; Armentrout, R. S.; Long, T. E. Macromolecules 2002, 35, 8738.
24. Zhang, X.; Tian, X. Y.; Zheng, K.; Zheng, J.; Yao, X. Y.; Li, Y.; Cui, P. J Macromol Sci Phys 2009, 47, 166.
25. Wellen, R. M. R.; Rabello, M. S. J Mater Sci 2005, 40, 6099.
26. Rabello, M. S.; White, J. R. Polymer 1997, 38, 6389.
27. Hieber, C. A. Polymer 1995, 36, 1455.
28. Qiu, Z.; Ikehara, T.; Nishi, T. Polymer 2003, 44, 5429.
29. Supaphol, P.; Dangseeyun, N.; Srimoaon, P.; Nithitanakul, M. Thermochim Acta 2003, 406, 207.
30. Wunderlich, B. Macromolecular Physics; Academic Press: New York, 1976; Vol. 2.
31. Huang, H.; Gu, L.; Ozaki, Y. Polymer 2006, 47, 3935.
32. Stoeffler, K.; Lafleur, P. G.; Denault, J. Polym Degrad Stab 2008, 93, 1332.
33. Schooten, J. V.; Hoorn, H. V.; Boerma, J. Polymer 1961, 2, 161.
34. Rabello, M. S. Ph.D Dissertation, Department of Mechanical, Materials and Manufacturing Engineering, University of Newcastle upon Tyne, 1996.
35. Gümther, B.; Zachmann, H. G. Polymer 1983, 24, 1008.